3D-EBP: A PROGRAMMABLE 3D BIONANORECEPTOR ASSEMBLY

Sangwook Chu[1,2], Ben Hurwitz[1], Thomas E. Winkler[2,3], Adam D. Brown[3,4], James N. Culver[3,4,5], and Reza Ghodssi[1,2,3]

[1]Department of Electrical and Computer Engineering, [2]Institute for Systems Research,
[3]Fischell Department of Bioengineering, [4]Institute for Bioscience and Biotechnology Research,
[5]Department of Plant Science and Landscape Architecture,
University of Maryland, College Park, USA

ABSTRACT

This paper presents a novel biofabrication technology utilizing electrowetting principles for localized 3-D functionalization of *Tobacco mosaic viruses* (TMVs) onto structurally hydrophobic micropillar arrays (μPAs). A custom-built 3-D electro-bioprinting (3D-EBP) system enables exquisite control over positioning and wetting of TMV solution onto the water repellent 3-D substrate. The 3D-EBP is evaluated using SEM and fluorescent labeling for characterization of TMV's nanostructured morphology and their biochemical activities, respectively. A complete yet localized assembly of TMVs on μPAs is confirmed in SEM. The increased density of TMVs per device foot-print (vs. TMVs on planar substrate) results in a significant 7-fold increase in fluorescence intensity attributed to the μPAs. On a single μPA substrate (7×7 mm^2), 3D-EBP of 3×3 hierarchical TMV arrays is demonstrated to emphasize the unique 3D patterning capability. Overall, the results confirm successful application of electrowetting principles for creating highly functional device components spanning the micro/nano/bio domains.

INTRODUCTION

Recently, a wide-range of biological materials (e.g. nucleic acids, peptides, antibodies, viruses, biopolymers, cells, etc.) has been integrated into micro/nano fabrication processes (or 3-D printing technologies) in efforts to create functional system components embedded with biological attributes (biological structures, biochemical activities, etc.) [1]. The advancement of these biofabrication processes has largely been driven by the increasing interest and need for miniaturized biosensors in point-of-care (POC) and lab-on-a-chip (LOC) systems toward decentralized, easy-to-use, and rapid monitoring/treatment of human health/disease.

Considering the size constraints on the desired system foot-print, three-dimensional micro/nano structures have been effectively utilized in a wide range of miniaturized systems by offering increased density of functional materials and interactive surfaces [2,3]. One of the most simple yet highly functional 3-D structure is the micropillar arrays (μPAs). Due to the many beneficial attributes offered by the 3-D structures – high surface-to-volume ratio, scalable geometrical features, highly ordered arrangement, and high reproducibility/reliability obtained by standardized microfabrication processes or 3-D printing technology – μPAs have widely been applied for the advancement in many miniaturized system components including micro energy storage devices [2,3], biochemical sensors [4], and micro-coolers [5].

In the past decade, our group and collaborators have been developing miniaturized device components (micro-energy storage devices and bio/chemical sensors) utilizing genetically-modified *Tobacco mosaic viruses* (TMVs) as a nanoscale functional material embedded in device components [2,3,6,7]. In our recent efforts to integrate TMVs with 3-D microstructures for creating hierarchically structured functional component, the structural hydrophobicity present in micropillar arrays was identified as a key limiting factor prohibiting introduction of TMVs into deep microcavities [8].

In this work, we present a novel biofabrication technology utilizing electrowetting principles [9] to enable uniform and arrayed functionalization of TMVs onto the μPAs. A custom-built 3-D electro-bioprinting (3D-EBP: electrowetting on 3D microstructures + bionanoreceptor assembly) system allows both rigorous control over positioning of the TMV solution on the water-repellent substrate and complete yet localized wetting of μPAs for 3-D functionalization. Our process evaluation results confirm the applicability of electrowetting principles for programmable biofabrication processes and the resulting functional components can potentially lead to the development of advanced microsystem components.

MATERIALS AND METHODS

Au-coated Si-μPAs and structural hydrophobicity

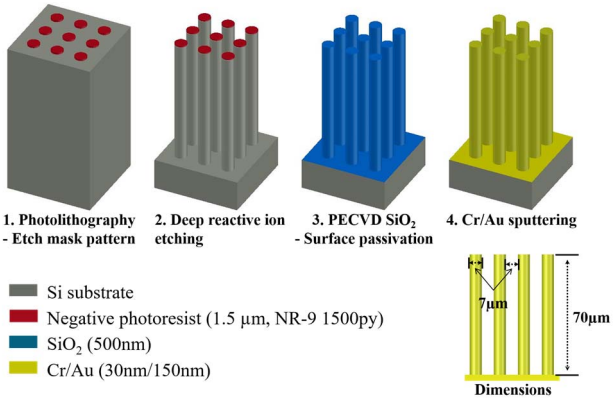

Figure 1: Fabrication process for the μPAs and the dimensions of the high-aspect-ratio microstructure.

The fabrication process for the μPAs is described in Figure 1. A Si wafer is etched down via DRIE using a photolithographically patterned negative photoresist (NR9-1500PY, Futurrex) as the etch mask. The resulting Si micropillar arrays are passivated by 500 nm PECVD SiO_2 followed by sputtering of Cr (30nm)/Au (150nm). The footprint of the final μPA substrate is 1×1 cm^2 with 10:1 aspect ratios for both pillars and spacings (pillar diameter and spacing between nearest pillars: 7μm, pillar height:

70µm). Such high-aspect-ratio geometry is selected to advance from our previous works [10]. Also, to our best knowledge, successful biofunctionalization on such high-aspect-ratio microstructures has never been reported previously.

Contact angle characterization of 10µl sessile drops of the TMV solution on planar Au (Figure 2a) and Au-coated µPA (Figure 2b) substrates is shown in Figure 2. While the planar Au surface exhibits hydrophilic nature with 65º contact angle, the µPAs results in hydrophobic characteristics with a 132º contact angle (*Cassie-Baxter* state). This is close to the theoretically expected value (136 º) calculated based on the *Cassie* equation (1), where θ* is the apparent contact angle on the µPAs, ϕ_s is the fraction of the solid in contact with the TMV solution, and θ_0 is the contact angle on the planar Au substrate.

$$\cos\theta^* = -1 + \phi_s (1 + \cos\theta_0) \quad (1)$$

Compared to our previous work on 7:1 spacing aspect-ratio geometries [10], the measured contact angle indicates reduced hydrophobicity (145º to 132º) due to the increased ϕ_s (0.133 to 0.196). However, it becomes more challenging to introduce the solution into the narrower cavities due to less pressure loading per each spacing segments (i.e. wider spacing reduces ϕ_s and increases the fraction of the liquid droplet that is supported by the pillars) [11]. The TMV droplets on the µPAs are readily movable with no traceable liquids remaining on the electrode surface.

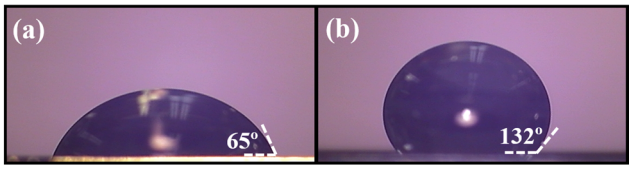

Figure 2: Contact angle measurements of 10µl sessile drops of TMV solution (0.2mg/ml in 0.1M phosphate buffer solution) on Au-coated (a) planar and (b) µPAs substrate.

3D-EBP: electro-bioprinting on 3-D µPAs

The term 3-D electro-bioprinting (3D-EBP) is introduced for the first time to represent the technology utilizing electrowetting for functionalization/self-assembly of biological materials (TMVs in this work) onto structurally hydrophobic µPAs. The word "printing" is used to reflect the system's "printer-like" operation when introducing the biological materials onto the µPA substrate. Figure 3a shows an overview of the 3D-EBP system comprised of six major elements; 1) TMV solution, 2) Au-coated Si µPAs, 3) stainless-steal nozzle coated with hydrophobic film (polyimide), 4) AC function generator, 5) XYZ micromanipulator, and 6) optical microscope. The 3D-EBP is conducted in air at room temperature. The details of each elements are described below.

The TMV solution in the 3D-EBP system functions as a biological ink to be printed/functionalized on the µPAs. The TMVs used in this work are genetically-modified with cysteine groups (-SH) on their surfaces. This allows for self-assembly onto Au surfaces through Au-thiol binding as well as uniform metallization over their nanoscale structure through electroless plating (details can be found at [12]). This is critical for the successful demonstration of this approach, allowing characterization of functionalization morphology and biochemical activity after the 3D-EBP process via SEM and fluorescent labeling.

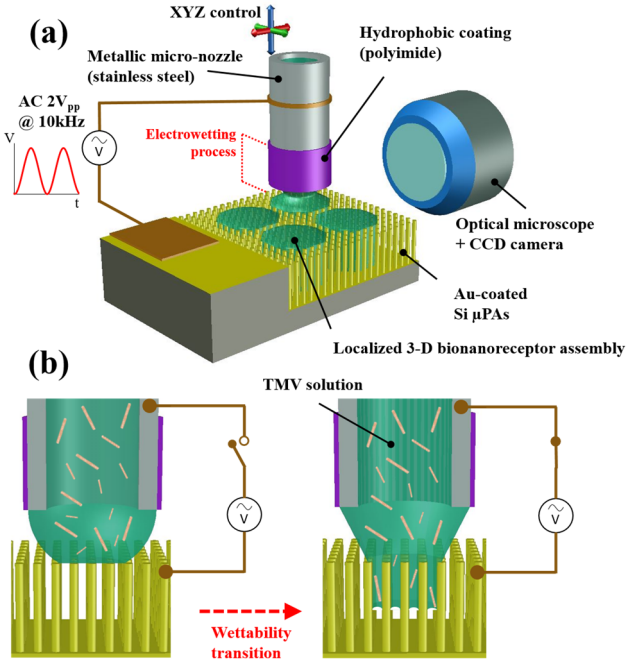

Figure 3: (a) An overview of the 3D-EBP process/control set-up and (b) cross-sectional schematics describing the electrowetting process.

The µPA substrate plays a role as 3-D substrate in 3D-EBP system. The hydrophobicity provides control capability to the wetting/printing process by limiting the substrate wetting at thermal equilibrium. The Au layer coated over the Si pillar structure functions as electrode for the electrowetting process as well as a means for the functionalization of the cysteine-modified TMVs through Au-thiol binding mechanism.

Considering the hydrophobicity of the substrate, it is challenging to accurately locate the TMV solution on the µPAs; more problematic when the volume of the solution reduces to micro-liters. This is overcome by the use of a modified metallic nozzle and the XYZ micromanipulator positioned over the substrate. Specifically, the hydrophobic film (polyimide) coating around the outer surface of the metallic nozzle enables formation of a semi-spherical hanging drop of the biological solution. This key modification allows precise control over the amount of the dispensed solution in each electrowetting step (~1µl/3D-EBP). Without the coating the dispensed liquid would immediately roll upward to the outer metallic surface which makes it challenging to control the size and amount of the solution required for the electrowetting step.

The electrowetting portion of the 3D-EBP is described in Figure 3b. As shown in the left figure, the TMV solution at the nozzle forms *Cassie-Baxter* state when it is loaded onto the µPAs. When the electrowetting voltage is applied, an instant transition in surface wettability is induced driving the TMV solution into the microcavities (Figure 3b, right, transitioning to *Wenzel* state). This allows uniform self-assemby/functionalization of TMVs onto the surfaces of the deep microstructures.

In order to apply the electrowetting voltage at the solid-liquid interface formed at the tip of the pillars, an AC function generator is directly connected to the µPAs and the stainless-steel part of the nozzle. With a step-wise increase in the applied voltage level (peak-to-peak voltage amplitude, V_{pp}), a subtle change in wettability transition was observed at around $1.5V_{pp}$ (data not shown). For sufficient and facile transition of the wetting state (*Cassie-Baxter* state to *Wenzel* state) $2V_{pp}$ is determined to be the working voltage. The frequency of the applied voltage is kept at 10kHz to minimize bubble generation from electrolysis of water.

RESULTS AND DISCUSSION

Characterization of localized electrowetting process

The electrowetting process is monitored using cross-sectional optical microscopies as shown in Figure 4. The time-lapse images in Figure 4a show the evolution of the TMV droplet configuration during the electrowetting process. When the $2V_{pp}$ at 10kHz is applied, an immediate change in contact angle – 143º to 122º – is observed indicating instantaneous breakdown of the structural hydrophobicity (note that the initial contact angle is measured different in this hanging droplet condition compared to the sessile drop shown in Figure 2b). Over the course of 15 seconds, the contact angle reaches a minimum of 71º which is close to the contact angle measured on a planar Au substrate (Figure 2a). This indicated the complete wetting of the µPAs with the TMV solution (*Wenzel* state) [9].

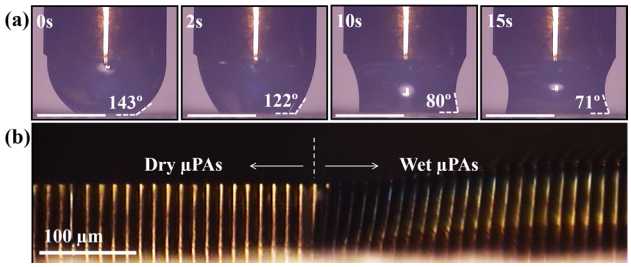

Figure 4: Optical microscope images showing (a) changes in contact angle and droplet configuration over the initial 15 seconds of the electrowetting step. (b) A clear wetting boundary observed in a magnified cross-sectional view of the µPAs. (scale bar: 1mm unless specified)

Figure 4b shows a magnified cross-sectional view of the micropillar arrays forming wetting boundary on a single micropillar surface at the wetting edge. This observation implies that the lateral access of the TMV solution is limited/controlled by the surface tension formed on the arrays of the pillar sidewalls allowing localized TMV functionalization on a single µPAs substrate. The complete wetting of the micropillar arrays can be confirmed on the right side of the image (where 3D-EBP was processed) while the left side of the pillars remain dried. Combined the 3D-EBP allows uniform patterning of the bionanoreceptor in three dimensional hierarchical arrangement using minimal amount of biological solution.

Morphology of TMVs after 3D-EBP

The hierarchical morphology of the TMV functionalized µPAs has been characterized via SEMs shown in Figure 5. Electroless Ni coating was performed following the previously reported protocol, which has been utilized for creating TMV-based nanostructured conductive materials [12]. The cross-sectional images taken from the 3D-EBP processed µPA substrates confirm complete and uniform TMV nanotexturing of the µPAs (Figure 5a). Compared to our previous methods using complete immersion of the substrates into 1ml TMV solution bath [8], this is a significant improvement considering the excellent uniformity of TMV coating at the lower portion of the µPA surfaces. Figure 5b shows the µPAs that are exposed to a TMV droplet without electrowetting. Only isolated TMVs are observed at the top surfaces of the pillars with most of the micropillar surfaces bare. This indicates that the *Casie-Baxter* state of the droplet is stable through the overnight self-assembly process and raises the significance of the 3D-EBP as an enabling technology.

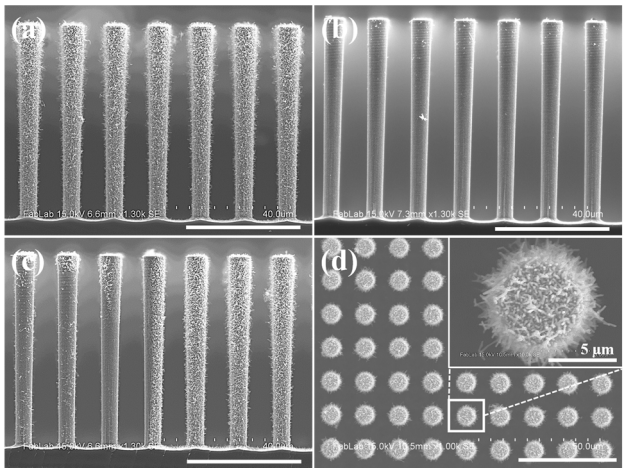

Figure 5: SEM images of the µPAs with nanostructured TMVs. (a) 3D-EBP allowed a complete TMV coverage along the deep micropillar side-walls compared to the (b) non-EBP processed µPAs. (c) A clear functionalization boundary formed along a single pillar surface at the wetting edge. (d) Top-down view of the µPAs showing a uniform TMV coverage across the 3D-EBP processed µPAs. (scale bars: 40 µm unless specified)

Figure 5c shows the µPAs located at the wetting edge. Corresponding with the optical microscope image shown in Figure 4b, a clear functionalization boundary is formed on a single sidewall. The initial limitation from the structural hydrophobicity plays an advantageous role to locally confine the bionanoreceptor functionalization on the high-surface-area substrate. With the addition of the top-down SEM images showing the TMV-based nanostructures on top surfaces, the morphology characterization results confirm applicability of the electrowetting principles for creating highly functional conductive hierarchical device structures.

Biochemical assay of TMV after 3D-EBP

Biochemical activity of the TMVs assembled by 3D-EBP is evaluated using a sulfhydryl (-SH) specific fluorescent labeling reagent, Fluorescein-5-Maleimide. Figure 6a and 6b compares the fluorescence emitted by the TMVs on planar Au (Figure 6a) and µPA (Figure 6b)

substrates. Fluorescent microscope settings were identical for both images (e.g. magnification, exposure time, etc.). As clearly observed, a significant increase in the fluorescence intensity is achieved with the 3D-EBP attributed to the increased nanoreceptor density within the functionalization area. The image analysis (ImageJ) results indicated ~7-fold increase of the intensity (Figure 6c). In efforts to demonstrate the patterning capability of 3D-EBP, 3×3 hierarchical TMV arrays on 7×7 mm^2 µPA substrate is fabricated as shown in Figure 6d. As indicated by the error bars in Figure 6c, the 3D-EBP processed TMV arrays show excellent uniformity in biochemical activity over the arrays of functionalized spots. The results emphasize the potential advantages of 3D-EBP for building multiplexed or high-throughput bio/chemical sensing/analysis platforms.

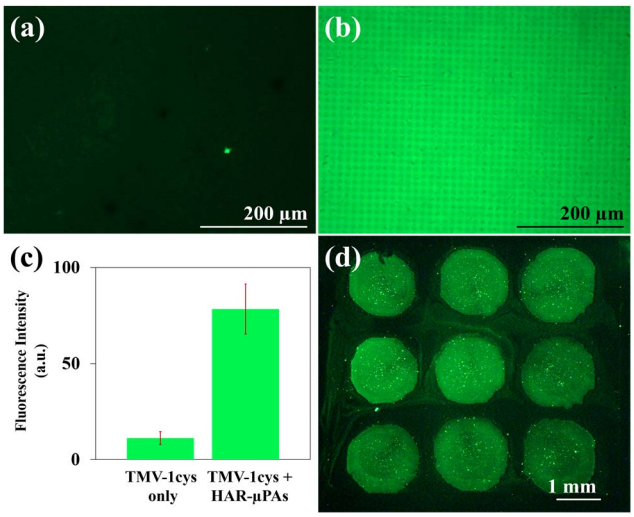

Figure 6: Fluorescent microscopy characterization confirming biochemical activity of TMVs after 3D-EBP. Comparing TMVs on (a) planar and (b) µPAs, (c) a 7-fold increase in fluorescence intensity is achieved (n=9) with excellent process uniformity across the (d) 3×3 arrays of hierarchical bionanoreceptors.

CONCLUSION

This work reports successful application of electrowetting principles in efforts to create highly functional micro/nano/bio integrated device/system components. The 3D-EBP introduced in this work enables complete functionalization of biological nanoreceptors onto structurally hydrophobic microstructured substrates. The potential scalability and programmability of the 3D-EBP opens up great opportunities in biofabrication technologies for creating highly functional bio-integrated devices. The simple principles, readily available system components, and the minimal volumes of biological solutions suits the major criteria for widespread application of this technology.

ACKNOWLEDGEMENTS

This work was funded by the Biochemistry Program of the Army Research Office (W911NF-14-1-0286). The authors would like to acknowledge the support of the Maryland Nanocenter and its FabLab for support in fabrication and imaging processes.

REFERENCES

[1] X. Z. Fan, E. Pomerantseva, M. Gnerlich, A. Brown, K. Gerasopoulos, M. McCarthy, J. Culver, and R. Ghodssi, "Tobacco mosaic virus: A biological building block for micro/nano/bio systems," *J. Vac. Sci. Technol. A*, vol. 31, no. 5, pp. 50815 (24), 2013.

[2] K. Gerasopoulos, E. Pomerantseva, M. McCarthy, A. Brown, C. Wang, J. Culver, and R. Ghodssi, "Hieararchical three-dimensional microbattery electrodes combining bottom-up self-assembly and top-down micromachining," ACS Nano, vol. 6, no. 7, pp. 6422–6432, 2012.

[3] S. Chu, K. Gerasopoulos, and R. Ghodssi, "Tobacco mosaic virus-templated hierarchical Ni/NiO with high electrochemical charge storage performances," *Electrochim. Acta*, vol. 220, pp. 184–192, 2016.

[4] F. Liu, Y. Piao, J. S. Choi, and T. S. Seo, "Three-dimensional graphene micropillar based electrochemical sensor for phenol detection," *Biosens. Bioelectron.*, vol. 50, pp. 387–392, 2013.

[5] S. Adera, D. Antao, R. Raj, and E. N. Wang, "Design of micropillar wicks for thin-film evaporation," *Int. J. Heat Mass Transf.*, vol. 101, pp. 280–294, 2016.

[6] F. Zang, K. Gerasopoulos, X. Z. Fan, A. D. Brown, J. N. Culver, and R. Ghodssi, "Real-time monitoring of macromolecular biosensing probe self-assembly and on-chip ELISA using impedimetric microsensors," *Biosens. Bioelectron.*, vol. 81, pp. 401–407, 2016.

[7] F. Zang, K. Gerasopoulos, X. Z. Fan, A. D. Brown, J. N. Culver, and R. Ghodssi, "An electrochemical sensor for selective TNT sensing based on Tobacco mosaic virus-like particle binding agents," *Chem. Commun.*, vol. 50, no. 85, pp. 12977–12980, 2014.

[8] S. Chu, K. Gerasopoulos, and R. Ghodssi, "Bio-nanotextured high aspect ratio micropillar arrays for high surface area energy storage devices," in *Digest Tech Papers PowerMEMS'15*, Boston, December 1-4, 2015, pp. 12065 (5pp).

[9] V. Bahadur and S. V Garimella, "Electrowetting-based control of static droplet states on rough surfaces," *Langmuir*, vol. 23, no. 9, pp. 4918–4924, 2007.

[10] S. Chu, F. Zang, A. D. Brown, J. N. Culver, and R. Ghodssi, "Localized bionanoreceptor 3D-assembly via electrowetting: An integrated micro/nano/bio fabrication technology," in *Digest Tech. Papers Hilton Head Workshop'16*, Hilton Head, June 5-9, 2016, pp. 157-160.

[11] A. Tuteja, W. Choi, M. Ma, J. M. Mabry, S. a Mazzella, G. C. Rutledge, G. H. McKinley, and R. E. Cohen, "Designing superoleophobic surfaces," *Science*, vol. 318, no. 5856, pp. 1618–1622, 2007.

[12] E. Royston, A. Ghosh, P. Kofinas, M. T. Harris, and J. N. Culver, "Self-assembly of virus-structured high surface area nanomaterials and their application as battery electrodes," *Langmuir*, vol. 24, no. 3, pp. 906–912, 2008.

CONTACT

*R. Ghodssi, tel: +1-301-405-8158; ghodssi@umd.edu